AMERICAN SOCIETY FOR MICROBIOLOGY | Journal of Virology®

VIRUS-CELL INTERACTIONS

Herpes Simplex Virus gE/gI and US9 Promote both Envelopment and Sorting of Virus Particles in the Cytoplasm of Neurons, Two Processes That Precede Anterograde Transport in Axons

Grayson DuRaine,[a] Todd W. Wisner,[a] Paul Howard,[a] Melissa Williams,[b] David C. Johnson[a]

Department of Molecular Microbiology & Immunology[a] and Multiscale Microscopy Core,[b] Oregon Health & Science University, Portland, Oregon, USA

ABSTRACT Herpes simplex virus (HSV) anterograde transport in neuronal axons is vital, allowing spread from latently infected ganglia to epithelial tissues, where viral progeny are produced in numbers allowing spread to other hosts. The HSV membrane proteins gE/gI and US9 initiate the process of anterograde axonal transport, ensuring that virus particles are transported from the cytoplasm into the most proximal segments of axons. These proteins do not appear to be important once HSV is inside axons. We previously described HSV double mutants lacking both gE and US9 that failed to transport virus particles into axons. Here we show that gE$^-$ US9$^-$ double mutants accumulate large quantities of unenveloped and partially enveloped capsids in neuronal cytoplasm. These defects in envelopment can explain the defects in axonal transport of enveloped virions. In addition, the unenveloped capsids that accumulated were frequently bound to cytoplasmic membranes, apparently immobilized in intermediate stages of envelopment. A gE-null mutant produced enveloped virions, but these accumulated in large numbers in the neuronal cytoplasm rather than reaching cell surfaces as wild-type HSV virions do. Thus, in addition to the defects in envelopment, there was missorting of capsids and enveloped particles in the neuronal cytoplasm, which can explain the reduced anterograde transport of unenveloped capsids and enveloped virions. These mechanisms differ substantially from existing models suggesting that gE/gI and US9 function by tethering HSV particles to kinesin microtubule motors. The defects in assembly of gE$^-$ US9$^-$ mutant virus particles were novel because they were neuron specific, in keeping with observations that US9 is neuron specific.

IMPORTANCE Herpes simplex virus (HSV) and other alphaherpesviruses, such as varicella-zoster virus, depend upon the capacity to navigate in neuronal axons. To do this, virus particles tether themselves to dyneins and kinesins that motor along microtubules from axon tips to neuronal cell bodies (retrograde transport) or from cell bodies to axon tips (anterograde transport). This transit in axons is essential for alphaherpesviruses to establish latency in ganglia and then to reactivate and move back to peripheral tissues for spread to other hosts. Anterograde transport of HSV requires two membrane proteins: gE/gI and US9. Our studies reveal new mechanisms for how gE/gI and US9 initiate anterograde axonal transport. HSV mutants lacking both gE and US9 fail to properly assemble enveloped virus particles in the cytoplasm, which blocks anterograde transport of enveloped particles. In addition, there are defects in the sorting of virus particles such that particles, when formed, do not enter proximal axons.

KEYWORDS neuron, glycoproteins, anterograde, envelopment, axons, kinesins

Received 9 January 2017 **Accepted** 14 March 2017

Accepted manuscript posted online 22 March 2017

Citation DuRaine G, Wisner TW, Howard P, Williams M, Johnson DC. 2017. Herpes simplex virus gE/gI and US9 promote both envelopment and sorting of virus particles in the cytoplasm of neurons, two processes that precede anterograde transport in axons. J Virol 91:e00050-17. https://doi.org/10.1128/JVI.00050-17.

Editor Richard M. Longnecker, Northwestern University

Address correspondence to David C. Johnson, johnsoda@ohsu.edu.

Following reactivation from latency, alphaherpesvirus particles move from neuron cell bodies into axons and then to the axon tips. This process is known as anterograde transport and involves transport by kinesin motors that facilitate fast axonal transport on microtubules (reviewed in reference 1). Anterograde transport is an indispensable process allowing large quantities of infectious virus to be produced in epithelial tissues as well as virus dissemination to other hosts.

Two herpes simplex virus (HSV) membrane proteins, namely, gE/gI, a heterodimer of the type I membrane glycoproteins gE and gI, and US9, a type II membrane protein (Fig. 1), play important roles in anterograde transport (reviewed in references 2 and 3). Much is known about how gE/gI functions in virus egress from polarized epithelial cells (reviewed in reference 2). gE- and gI-null mutants spread poorly in epithelial tissues and between polarized epithelial cells in culture (4–6). In the nervous system, retinal gE/gI promotes both spread between retinal epithelial cells and neurons and spread in the nervous system in the anterograde direction, from the retina to the brain (7, 8). HSV US9 does not play an obvious role in virus spread in epithelial tissues but is important for anterograde spread in the nervous system (9) and for spread between cultured neurons and other cells (10). All of the studies with HSV and studies involving the related porcine alphaherpesvirus pseudorabies virus (PRV) suggest that gE/gI and US9 in neurons promote anterograde spread of virus but not its retrograde spread (1, 2, 7, 11–18).

The HSV gE/gI and US9 proteins differ from their PRV homologues. The PRV US9 protein is largely essential for anterograde transport in the axons of cultured neurons (15, 19), while HSV US9-null mutants show only about 40 to 50% reductions in HSV capsids and glycoproteins in distal axons (13, 20). In contrast, HSV double mutants lacking both gE and US9 are profoundly defective for anterograde transport of HSV glycoproteins, unenveloped capsids, and enveloped virions, exhibiting $<$5% of the capsids and glycoprotein puncta in proximal axons (17). Therefore, gE/gI and US9 act in a synergistic or cooperative fashion to promote anterograde transport.

Observations that very few capsids and glycoproteins were present in the most proximal sections of axons of neurons infected with the gE$^-$ US9$^-$ double mutant (17) suggested that gE/gI and US9 function at the very earliest stages of anterograde transport. Anterograde transport appears to be initiated by the loading of HSV and PRV particles onto kinesin motors (reviewed in references 15, 21, and 22). Since this process was severely inhibited in neurons infected with gE$^-$ US9$^-$ double mutants, it appeared that gE/gI and US9 cooperate in some fashion in the cytoplasm of neurons to begin the first stages of transport into axons. Selection of cellular cargo molecules that are transported into axons is a specific process involving direct or indirect interactions between cargo molecules and kinesins, which also bind microtubules (23–25). The hypothesis that gE/gI and US9 do not play a role in fast axonal transport within axons was suggested by experiments characterizing the very few capsids that were transported into axons following infection with an HSV gE$^-$ US9$^-$ double mutant. These capsids moved with normal velocities and without stalling (17). Similar results were observed in neurons infected with a PRV US9$^-$ mutant (16).

We can conceive of two potential mechanisms for how HSV gE/gI and US9 function in the cytoplasm of neurons to promote entry of virus particles into proximal axons. First, gE/gI and US9 may bind kinesins to initiate this transport. PRV US9 binds to kinesin-3 (KIF1A), PRV capsids colocalize with kinesin-3 in axons, and, importantly, dominant negative KIF1A reduces PRV capsid transport in axons (15). There is also evidence that PRV gE/gI is necessary for US9 binding to KIF1A (18). There have been reports that HSV US9 and the tegument protein US11 bind a different kinesin, kinesin-1 (classic kinesin), in bacterial pulldown experiments (22, 26). However, there have been no studies showing the functional relevance of kinesin-1 proteins in HSV anterograde transport.

A second model for how gE/gI and US9 might function suggests that these proteins organize the assembly of tegument with capsids and of capsids with envelopes and the intracellular sorting of virus particles into axons. Consistent with an effect on assembly,

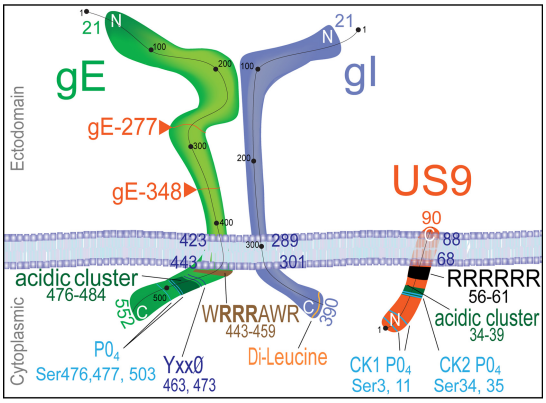

FIG 1 Cartoon of the structures of gE/gI and US9. The gE and gI polypeptides form a heterodimer, and the vast majority of gE and gI in infected cells is present in this form. gE and gI are type I membrane proteins with 300- to 400-amino-acid (aa) extracellular domains (top) and 90- to 110-aa cytoplasmic domains. US9 is a type II membrane protein with few extracellular sequences and a 67-aa cytoplasmic domain. The cytoplasmic domains of gE/gI and US9 would be most likely to determine sorting in membranes and contain a number of well-characterized TGN sorting sequences, including acidic clusters, tyrosine motifs, casein kinase 1 and 2 motifs, and dileucine motifs.

HSV mutants lacking gE, gI, or gE and gD exhibit defects in secondary envelopment (27, 28). gE/gI traffics specifically to the *trans*-Golgi network (TGN) by virtue of TGN sorting motifs in the gE and gI cytoplasmic domains (Fig. 1) (29–31). This sorting to the TGN increases the binding of tegument proteins to these membranes, and *vice versa* (32), apparently leading to enhanced envelopment there (reviewed in reference 2). In the TGN, enveloped virus particles are sorted specifically to epithelial cell-cell junctions (6, 30). Loss of gE/gI or the cytoplasmic domains of these proteins compromises this directed sorting of virus particles to junctions such that virus particles are directed to apical cell surfaces (6, 28–30, 32). Given that neurons are also highly polarized cells, gE/gI might also act in assembly and intracellular sorting to promote anterograde transport in axons. There is no evidence that HSV US9 acts to sort virus particles in epithelial cells. However, like gE and gI, US9 has a relatively large cytosolic domain that is laden with recognizable TGN sorting sequences (Fig. 1) (28, 33).

In the present study, we characterized the assembly and egress of HSV particles in neurons infected with HSV mutants lacking both gE and US9. There were major defects in assembly of enveloped particles in these neurons, suggesting that gE/gI and US9 act to promote secondary envelopment in the cytoplasm. In addition, there was evidence of defective sorting of virus particles in the cytoplasm of infected neurons. The loss of gE and US9 produced neuron-specific effects on virus assembly and sorting.

RESULTS

Rat embryonic SCG neurons infected with an HSV gE⁻ US9⁻ double mutant show more capsids that accumulate in the cytoplasm at early and intermediate times. The defects associated with loss of both HSV gE and US9 appear to occur in neuronal cell bodies, not in axons. To attempt to understand these cytoplasmic defects, we imaged neuronal cell bodies following infection with wild-type (WT) GS2483, a virus that expresses VP26-mRFP (producing red capsids) and gB-GFP (producing green glycoprotein) (34), or infection with a GS2483 derivative lacking both gE and US9 (denoted GS gE⁻ US9⁻ here) (17). After 7 or 14 h, the cells were fixed and imaged by deconvolution immunofluorescence microscopy. Surprisingly, there were substantially larger numbers of cytoplasmic capsids in superior cervical ganglion (SCG) neurons infected with GS gE⁻ US9⁻ than in neurons infected with wild-type GS2483 after both 7 h and 14 h (Fig. 2). Counts of fluorescent capsids in sections of SCG neurons by use of IMARIS software showed that there were, on average, 32 capsids in neurons infected with wild-type GS2483 after 7 h and 111 capsids in the cytoplasm of GS gE⁻ US9⁻ virus-infected SCG neurons at this time. After 14 h of infection, there was an average of

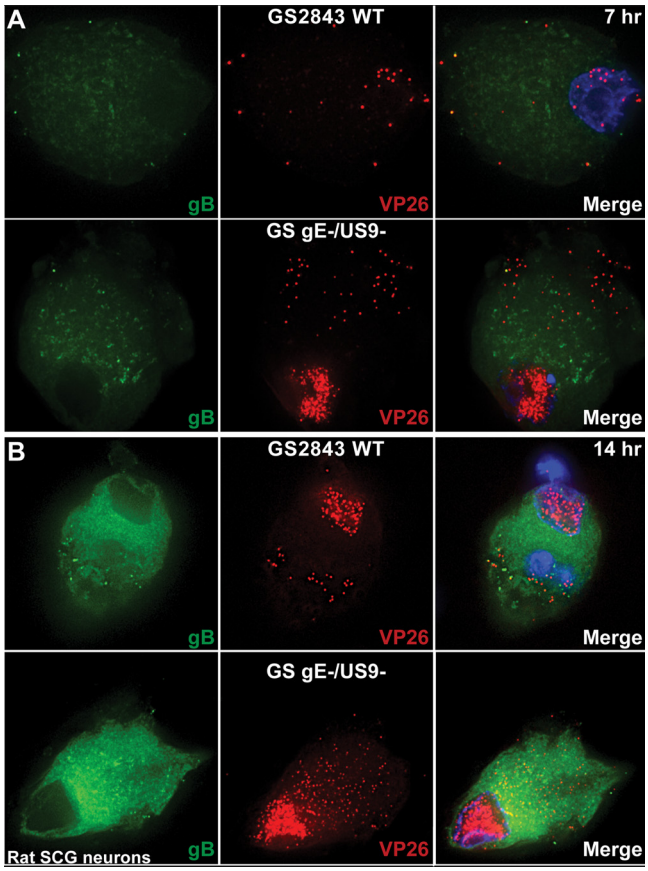

FIG 2 Immunofluorescence imaging of HSV capsids and gB in rat embryonic SCG neurons. Rat SCG neurons grown on polylysine/laminin-coated glass coverslips were infected with wild-type (WT) HSV GS2843 expressing gB-GFP and the capsid protein VP26-RFP or with a derivative of this virus lacking both the gE and US9 genes (GS gE$^-$ US9$^-$) at 8 PFU/cell. Cells were fixed with paraformaldehyde after 7 or 14 h and then permeabilized, and nuclei were stained with 300 nM DAPI. At 7 h (A) and 14 h (B), substantially more cytoplasmic capsids were observed with GS gE$^-$ US9$^-$ than with wild-type GS2843.

350 capsids in the cytoplasm of GS gE$^-$ US9$^-$ virus-infected SCG neurons and 77 capsids in wild-type GS2483-infected neurons. A large fraction (>50%) of the capsids that accumulated in the cytoplasm of GS gE$^-$ US9$^-$ virus-infected cells appeared to be unenveloped capsids, as there was little gB staining overlapping the capsid staining (Fig. 2). However, we did not attempt to enumerate unenveloped versus enveloped capsids given the relatively uniform distribution of gB in the cytoplasm of SCG neurons, and the studies described below address this question better. These observations were indeed surprising, and it was not clear how two membrane proteins, gE/gI and US9, could influence the number of cytoplasmic capsids, i.e., whether they did so by acting to increase capsid protein synthesis, capsid assembly, or intracellular trafficking of capsids.

Capsids that accumulated at these early times, especially at 7 h postinfection, would not be transported into axons, as transport into axons does not begin before 14 h in these neurons (17, 35). Thus, it did not seem possible that the capsids that accumulated to higher levels at 7 and 14 h resulted from defects in anterograde transport. As in our previous studies (17), the anterograde transport of the gE$^-$ US9$^-$ double mutant was blocked in these neurons, by ~95%. We counted capsids in axons of 5 wild-type GS2483-infected SCG neurons, and there was an average of 21 capsids in the proximal axons, whereas there was an average of 2.3 capsids/axon in GS gE$^-$ US9$^-$ virus-infected neurons. In studies related to these findings, we also imaged the axons of SCG neurons to ascertain whether the capsids in axons were unenveloped or enveloped (17, 35). Approximately half of the capsids in wild-type GS2483-infected neuronal axons were

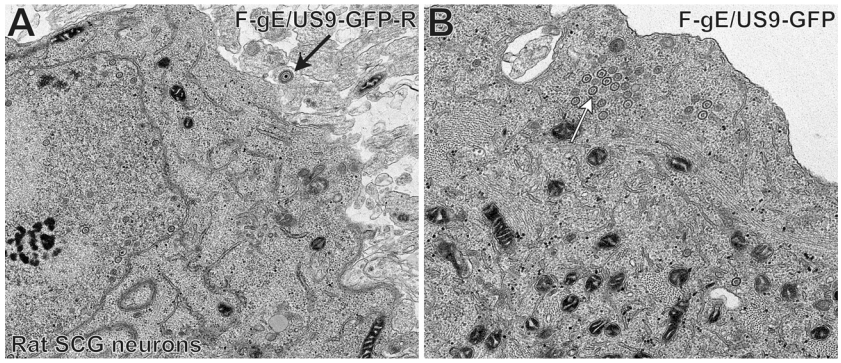

FIG 3 Electron micrographs of rat SCG neurons infected with the HSV F-gE/US9-GFP double mutant or the repaired virus, F-gE/US9-GFP-R. Rat SCG neurons were grown on polylysine/laminin-coated Thermanox plastic coverslips and infected with the repaired virus (F-gE/US9-GFP-R) (A) or the double mutant lacking gE and US9 (F-gE/US9-GFP) (B) for 18 h. SCG neurons were then fixed and processed for electron microscopy. The black arrow in panel A indicates an enveloped virion on the cell surface, and the white arrow in panel B indicates unenveloped capsids.

unenveloped, and half were enveloped. For example, 56 of a total of 111 capsids in the axon of the wild-type GS2483-infected SCG neuron shown in Fig. 2 were unenveloped, i.e., we detected no gB-GFP associated with VP26-mRFP capsids. The data supported the existence of a substantial fraction of unenveloped particles in axons of SCG neurons, as we reported previously (35).

We performed electron microscopic (EM) experiments to further characterize the substantial accumulation of HSV capsids in SCG neurons infected with the gE⁻ US9⁻ double mutant. These experiments focused on a different gE⁻ US9⁻ double mutant, F-gE/US9-GFP, in which the adjacent gE and US9 genes were replaced with green fluorescent protein (GFP) sequences, and a repaired version of this mutant, F-gE/US9-GFP-R, was produced (17). We found that F-gE/US9-GFP-R replicated better than wild-type GS2843, producing more infectious virus and more capsids, and this benefited the EM experiments. In SCG neurons infected with the repaired virus, we observed examples of enveloped virions on cell surfaces (Fig. 3A, black arrow). In SCG neurons infected with the F-gE/US9-GFP double mutant, there were many fewer enveloped particles at the cell surface and examples of unenveloped capsids in the cytoplasm (Fig. 3B, white arrow). However, the numbers of unenveloped and enveloped capsids in SCG neurons were small compared to those in our previous EM studies involving Vero, HaCaT, and HEC-1A cells (6, 27, 36). Thus, producing counts of different types of particles was difficult.

Immunofluorescence characterization of gE⁻ US9⁻ mutant-infected CAD neurons. We extended these studies to other neurons. CAD cells are derivatives of a mouse catecholaminergic central nervous system cell line that can be differentiated to become neurons and have been used to characterize anterograde and retrograde transport of HSV and PRV (34). Differentiated CAD neurons were infected with wild-type GS2483 or GS gE⁻ US9⁻. After 15 h of infection, we observed a substantial accumulation of capsids in the cytoplasm of CAD cells infected with GS gE⁻ US9⁻, but there were fewer capsids evident in the cytoplasm of neurons infected with the repaired wild-type GS2483 virus (Fig. 4A). In these images, it is important to differentiate between the very large numbers of capsids accumulated in the nucleus (where gB is not present; indicated by white arrows) and the capsids in the cytoplasm, marked by the presence of gB. In the 15-h merge images, there was largely green fluorescence (gB) in the cytoplasm and little red fluorescence (capsids) with wild-type GS2483, but there were recognizable capsids in the cytoplasm of GS gE⁻ US9⁻ virus-infected CAD cells. In the 18-h samples, there was a more pronounced difference, as many more capsids accumulated in the cytoplasm of GS gE⁻ US9⁻ virus-infected cells than in the cytoplasm of GS2483-infected cells (Fig. 4B). Counts of capsids in thin optical sections of the

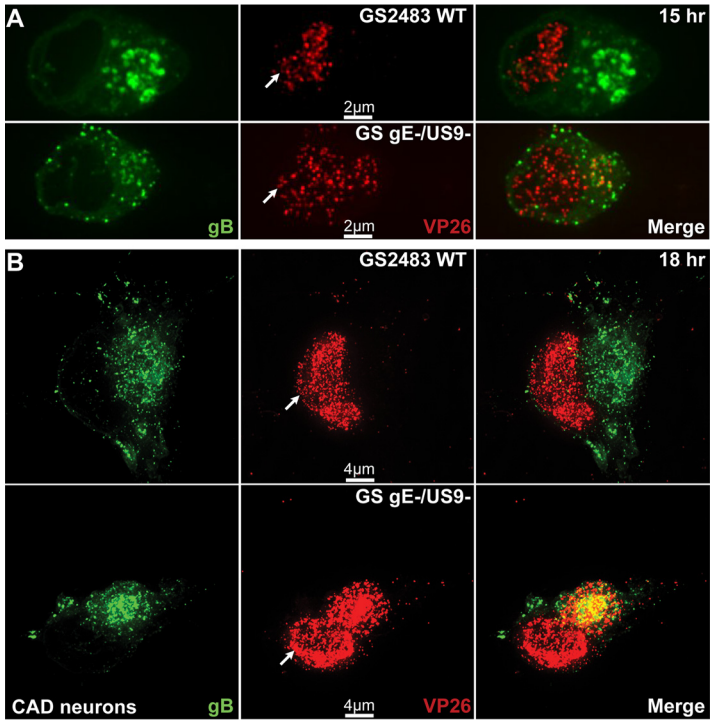

FIG 4 Immunofluorescence imaging of capsids and gB in CAD neurons infected with wild-type HSV GS2843 or with GS gE$^-$ US9$^-$. CAD neurons growing on polylysine/laminin-coated glass coverslips were differentiated for 8 days, infected with wild-type GS2843 expressing gB-GFP and VP26-RFP or with GS gE$^-$ US9$^-$ at 8 PFU/cell, and fixed with 4% paraformaldehyde at 15 h and 18 h postinfection. At 15 h (A) and 18 h (B), more cytoplasmic capsids accumulated in the cytoplasm of CAD cells infected with the GS gE$^-$ US9$^-$ double mutant than in that of WT GS2843-infected cells. White arrows in the VP26 column indicate the position of the nucleus. Note that the yellow color in the merged panels is not representative of colocalization but resulted from the flattened z-stacks used to produce the image.

cytoplasm of 6 cells infected with GS gE$^-$ US9$^-$ showed 2,325 capsids, whereas there were 270 capsids in the cytoplasm of 6 CAD cells infected with GS2843 WT. The density of the gB staining of membrane vesicles in the cytoplasm of GS2843 WT-infected cells made it very difficult to discern whether these capsids were enveloped or nonenveloped capsids.

As with SCG neurons, capsids and enveloped HSV particles did not enter CAD axons efficiently following infection with F-gE/US9-GFP compared to that with F-gE/US9-GFP-R (Fig. 5). There was >90% inhibition of capsids entering axons of F-gE/US9-GFP-infected CAD cells compared to those entering axons of F-gE/US9-GFP-R-infected CAD cells. Again, in the images, there is an extensive accumulation of capsids in the cytoplasm of F-gE/US9-GFP-infected neurons compared to that of F-gE/US9-GFP-R-infected neurons. Interestingly, we observed mostly enveloped virions in CAD axons. Counts showed that 8 of 110 (7.3%) capsids produced by WT GS2843 and 7 of 111 (6.3%) capsids produced by F-gE/US9-GFP-R were unenveloped, as assessed by the absence of detectable gB. These results showed a clear difference between the mostly enveloped virions in CAD neurons and the unenveloped capsids in SCG and SK-N-SH neurons (17, 35, 37, 38).

Electron microscopic analyses of CAD cells infected with the gE$^-$ US9$^-$ double mutant. CAD neurons infected with F-gE/US9-GFP or F-gE/US9-GFP-R were characterized by EM analyses. F-gE/US9-GFP-R produced primarily enveloped particles that were on cell surfaces (Fig. 6A and B). As shown in Fig. 6B and C, there were some capsids apparently in the process of envelopment, but again, most capsids were fully enveloped and on cell surfaces. Counts of 12 to 15 representative cells infected with F-gE/US9-GFP-R showed that the majority of capsids that had undergone egress beyond the nuclear envelope were fully enveloped and present on cell surfaces (Table 1).

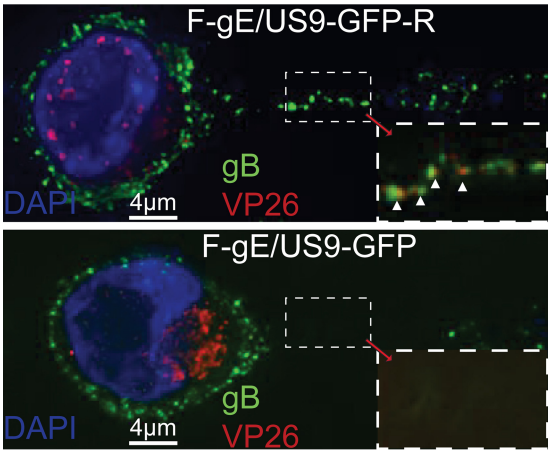

FIG 5 Immunofluorescence imaging of CAD neuron axons. CAD neurons growing on polylysine/laminin-coated glass coverslips were differentiated for 9 days and then infected with HSV F-gE/US9-GFP-R, in which the gE and US9 genes were repaired, or with the F-gE/US9-GFP double mutant lacking gE and US9, at 8 PFU/cell. At 18 h postinfection, the cells were fixed with 4% paraformaldehyde, permeabilized, immunostained with antibodies specific for HSV gB (green) and VP26 (red), and also stained with 300 nM DAPI (blue). CAD cells infected with F-gE/US9-GFP exhibited many capsids in the cytoplasm and very few or no capsids in the axon, whereas neurons infected with F-gE/US9-GFP-R showed few cytoplasmic capsids and capsids in axons. White arrowheads point to enveloped (married) virions in axons.

In contrast, F-gE-/US9-GFP produced primarily unenveloped or partially enveloped capsids that were not on cell surfaces (Fig. 7A to C). These capsids were distributed relatively uniformly throughout the cytoplasm. This was unlike the distribution of capsids produced by an HSV gD⁻ gE⁻ double mutant, which showed an accumulation of large aggregates including hundreds of capsids apparently glued together by tegument (27). With the gE⁻ US9⁻ mutant, the capsids that accumulated were largely separate from one another (Fig. 7B and C, asterisks). We also frequently observed capsids in partial stages of envelopment on the surfaces of tubular membranes (Fig. 7B and C, black arrows). Counts of capsids in F-gE/US9-GFP-infected CAD neurons showed a 10-fold decrease in cell surface enveloped particles, a 12-fold increase in unenveloped capsids, and a 6-fold increase in partially enveloped capsids compared to those of the repaired virus, F-gE/US9-GFP-R (Table 1). These partially enveloped capsids often appeared to be interrupted during the envelopment process. We did not provide standard deviations for the data in Table 1 and elsewhere because HSV-infected cells exhibited large differences (as much as 10-fold) in the total number of capsids per F-gE/US9-GFP-R-infected cell. That said, when we focused on cell-cell junctions of cells by adding together multiple sections to form a large stack of images, we could highlight cell-cell junctions where cell surface virions tended to accumulate. Cell-cell junctions can be seen by the accumulation of fluorescent gB. F-gE/US9-GFP-R exhibited capsid accumulation at these cell-cell junctions, as seen by a green line between cells (Fig. 8A, white arrow). In contrast, F-gE/US9-GFP-infected CAD cells did not show this accumulation (Fig. 8B). Therefore, the ~10-fold reductions of enveloped virions on cell surfaces of neurons infected with the gE⁻ US9⁻ double mutant were entirely explained by ~10-fold increases in cytoplasmic unenveloped capsids.

To characterize whether these differences would translate into a reduced amount of infectious virus, CAD cells were infected with F-gE/US9-GFP-R or F-gE/US9-GFP, and then the cells and cell culture medium were harvested together at various times. After infection for 12, 15, and 18 h, the gE⁻ US9⁻ double mutant produced 3.6-, 6.5-, and 5.2-fold less infectious virus, respectively, than that produced by the repaired virus (Fig. 9). The reductions of 5- to 7-fold were smaller than would be expected given that there were ~10-fold increases in unenveloped capsids observed by EM (Table 1). There may have been a small fraction of nonneuronal undifferentiated CAD cells in these cultures that produced abundant quantities of infectious virus.

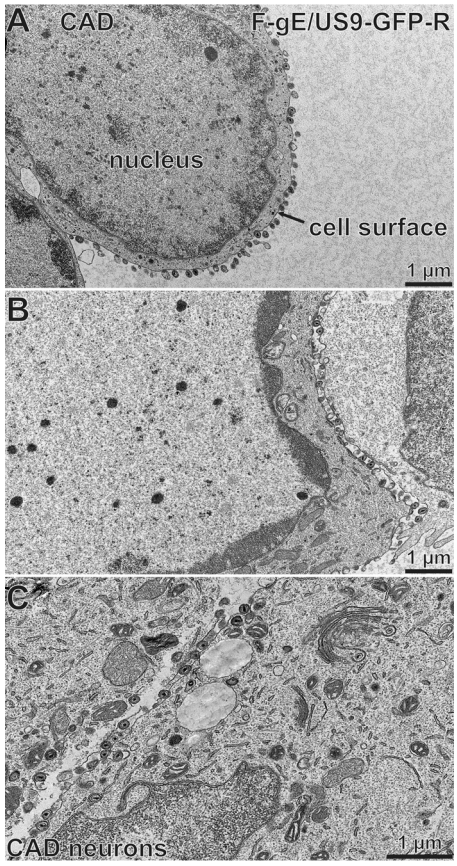

FIG 6 Electron micrographs of CAD neurons infected with the repaired HSV strain F-gE/US9-GFP-R. CAD neurons growing on collagen-coated 60-mm dishes were differentiated for 7 days and then infected with the repaired virus, F-gE/US9-GFP-R, at 20 PFU/cell for 18 h. The cells were then fixed and processed for electron microscopy. The majority of the capsids were enveloped and on cell surfaces. The cell surface and nucleus are indicated in panel A.

Defects in SK-N-SH human neurons. The EM experiments were extended to SK-N-SH neuroblastoma cells, which can be differentiated to produce axons, though they tend to be shorter than those of primary neurons. gE$^-$ and US9$^-$ mutants exhibit defects in axonal transport in SK-N-SH neurons (13, 37). Differentiated SK-N-SH cells infected with F-gE/US9-GFP-R displayed numerous cell surface virions, and there were fewer cytoplasmic enveloped or unenveloped capsids (Fig. 10A and B; Table 2). In contrast, SK-N-SH cells infected with the gE$^-$ US9$^-$ double mutant F-gE/US9-GFP showed primarily cytoplasmic, unenveloped capsids and partially enveloped capsids or capsids nestled up against tubular membranes (Fig. 11A and B; Table 2). The only real difference between these results for SK-N-SH neurons and those for CAD neurons was that, in SK-N-SH cells, capsids were frequently attached to tubular membranes without much wrapping of these around the capsids. There were also examples of capsids stuck

TABLE 1 Cytoplasmic and cell surface distribution of capsids produced by the gE$^-$ US9$^-$ double mutant F-gE/US9-GFP in CAD neurons[a]

Virus	No. of capsids (% of all capsids)			
	Unenveloped cytoplasmic	Partially enveloped cytoplasmic	Enveloped cytoplasmic	Cell surface virion
F-gE/US9-GFP-R	52 (4.9)	38 (3.6)	121 (11)	843 (80)
F-gE/US9-GFP	678 (58)	253 (22)	140 (12)	94 (8.1)

[a]EM images of 12 to 15 HSV-infected cells (that possessed large numbers of capsids) were analyzed by counting and characterizing the capsids.

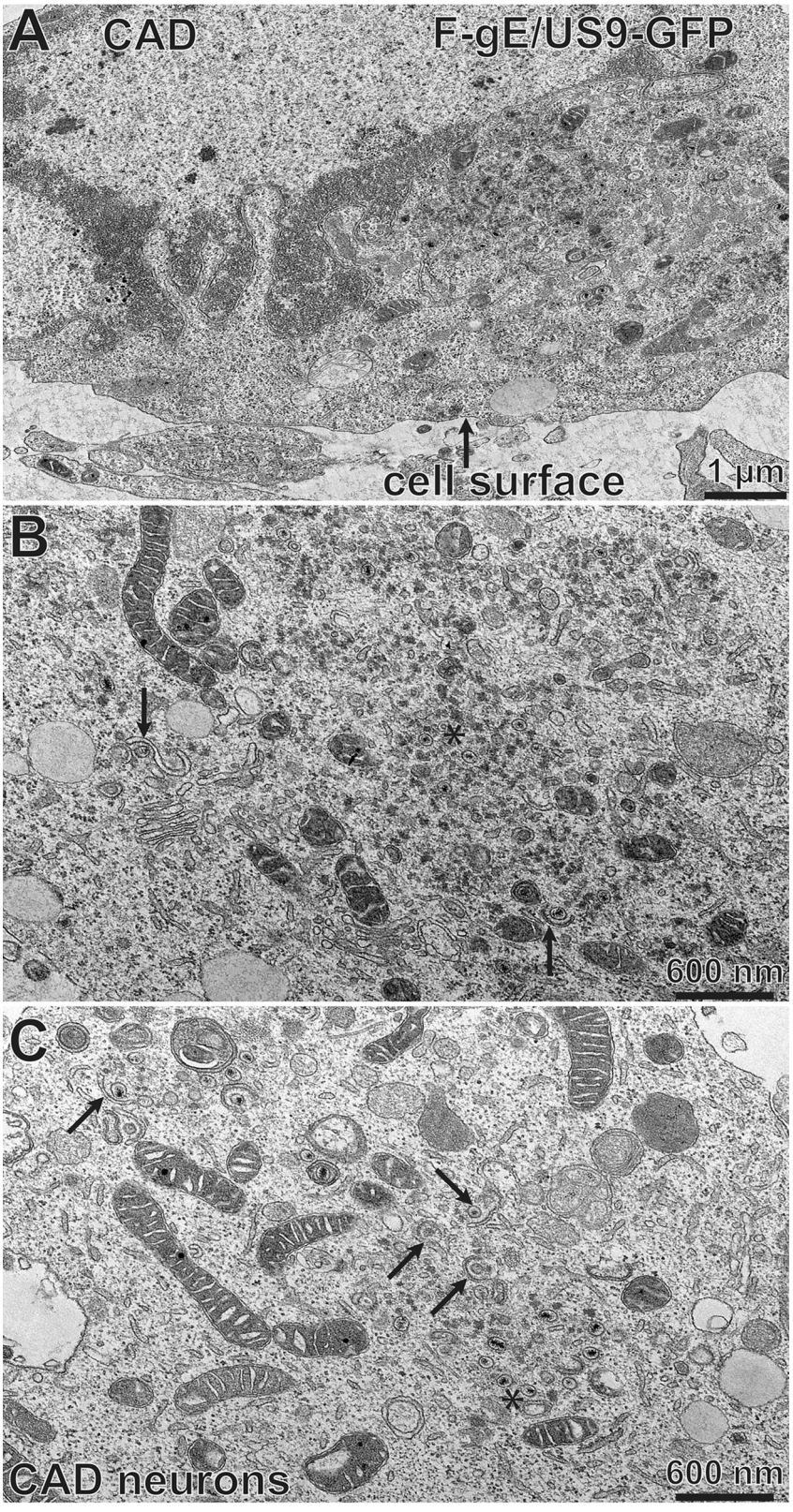

FIG 7 Electron micrographs of CAD neurons infected with the HSV F-gE/US9-GFP double mutant. CAD neurons growing on collagen-coated 60-mm dishes were differentiated for 7 days, infected with the F-gE/US9-GFP double mutant at 20 PFU/cell for 18 h, and then fixed and processed for electron microscopy. CAD neurons infected with F-gE/US9-GFP exhibited few enveloped virions on the cell surface (A) and numerous unenveloped (asterisks in panels B and C) and partially enveloped (black arrows in panels B and C) capsids in the cytoplasm. The cell surface is indicated in panel A.

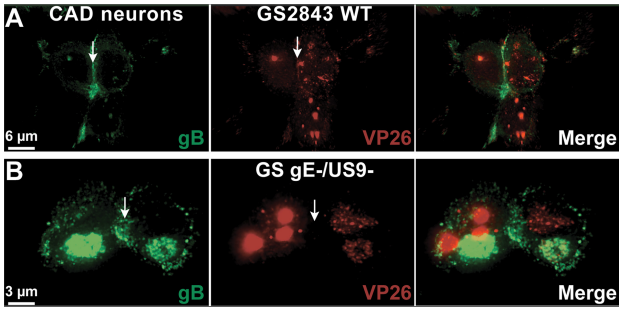

FIG 8 Immunofluorescence imaging of CAD neurons infected with GS2843 or GS gE$^-$ US9$^-$, focusing on cell-cell junctions. CAD neurons growing on polylysine/laminin-coated glass coverslips were differentiated for 10 days and then infected with WT GS2843 expressing gB-GFP and VP26-RFP (A) or with the gE$^-$ US9$^-$ version of this virus (GS gE−/US9−) (B) for 18 h. The cells were then fixed with 4% paraformaldehyde and analyzed by confocal microscopy. For these images, 16 separate 0.2-μm confocal sections were stacked together into a flattened image to attain images of cell-cell junctions. Numerous capsids accumulated at cell-cell junctions (white arrows) in cells infected with WT GS2843, but this was not the case for cells infected with the GS gE$^-$ US9$^-$ double mutant.

to what resembled Golgi stacks (Fig. 11A, asterisk). Thus, secondary envelopment was substantially blocked in F-gE/US9-GFP-infected SK-N-SH neurons.

Effects of deletion of single membrane proteins gE and US9 on HSV secondary envelopment in CAD cells. To determine how the individual membrane proteins gE and US9 contributed to the phenotypes described above, we characterized F-gEβ, a mutant HSV strain lacking just gE (4), and F-US9-GFP, a mutant lacking just US9 (9). CAD cells infected with the repaired HSV strain, F-gE/US9-GFP-R, displayed primarily (88%) cell surface virions (Fig. 12A; Table 3). Similar observations were observed with F-gEβ-R, a repaired version of the gE-null mutant, and F-US9-GFP-R, a repaired version of F-US9-GFP (not shown). Again, most (85%) of the postnuclear capsids in CAD cells infected with the F-gE/US9-GFP double mutant were unenveloped or partially enveloped cytoplasmic capsids, and there were few enveloped capsids on cell surfaces (Fig. 12B; Table 3). Many of the capsids scored as unenveloped were frequently bound to the surfaces of membranes (Fig. 12B, white arrow). CAD neurons infected with the US9-null mutant, F-US9-GFP, showed defects in secondary envelopment, as there was an accumulation of unenveloped capsids (Fig. 12D, white arrow). In addition, there were dense cytoplasmic membranes that often contained multiple capsids in the cytoplasm, and these enveloped particles frequently appeared to be malformed (Fig. 12C and D, black arrows). Significantly, many US9-null mutant-

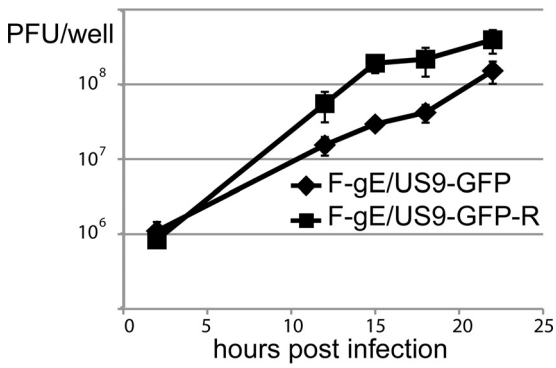

FIG 9 Production of infectious virus following infection of CAD neurons with an HSV double mutant (F-gE/US9-GFP) or repaired virus (F-gE/US9-GFP-R). CAD neurons were grown on polylysine/laminin-coated 6-well (10 cm^2) dishes and then differentiated for 7 days. The cells were infected (in triplicate) with F-gE/US9-GFP or the repaired virus (F-gE/US9-GFP-R) at 20 PFU/cell for 2 h and then washed extensively and incubated for 2, 8, 12, 18, or 22 h. The combined cells and culture media were collected and sonicated, and the amount of infectious virus was determined by plaque titration on Vero cells.

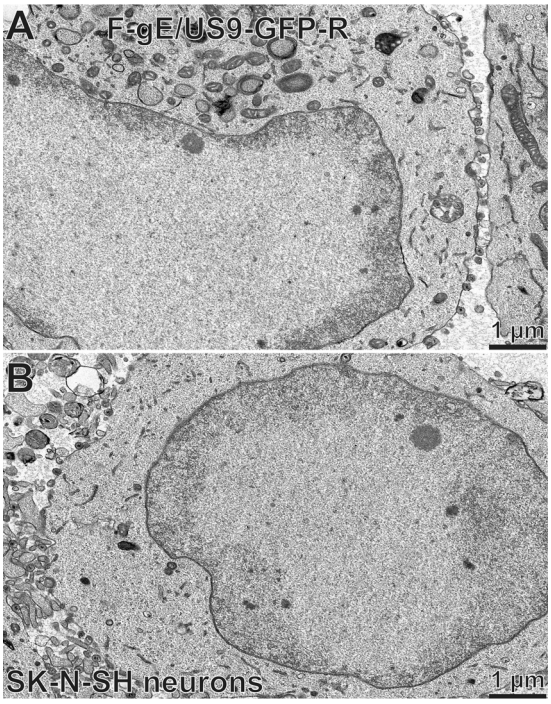

FIG 10 Electron micrographs of SK-N-SH neurons infected with the repaired HSV strain F-gE/US9-GFP-R. (A and B) SK-N-SH neurons growing on collagen-coated 60-mm dishes were differentiated for 10 days and then infected with the gE/US9-repaired virus F-gE/US9-GFP-R at 5 PFU/cell for 18 h. The cells were fixed and processed for electron microscopy. SK-N-SH neurons infected with F-gE/US9-GFP-R exhibited numerous enveloped virions on cell surfaces.

infected cells exhibited numerous cell surface virions, though not equaling the numbers observed with repaired viruses (Fig. 12C; Table 3). CAD cells infected with the gE-null virus, F-gEβ, displayed large numbers of enveloped capsids that appeared to be normal and in the cytoplasm (Fig. 12E and F, black arrows), amounting to 67% of the postnuclear capsids, and there were fewer cell surface virions (Table 3). We concluded that loss of US9 alone had only modest effects on HSV envelopment in CAD cells, as cell surface particles were reduced by only ~40%. Loss of gE had a much more substantial effect, as fully enveloped virions accumulated in the cytoplasm and did not reach cell surfaces.

Effects of deletion of gE or US9 or both gE and US9 on virus assembly in nonneuronal cells. To determine whether the effects of US9 and gE/gI were neuron specific, we performed EM studies involving HaCaT cells (human keratinocytes). Again, there were primarily cell surface particles with the repaired virus, F-gE/US9-GFP-R (Fig. 13A; Table 4). There were 2- to 3-fold increases in the numbers of unenveloped, partially enveloped, and enveloped particles in the cytoplasm of HaCaT cells infected with the F-gE/US9-GFP double mutant (Fig. 12B and C and 13B [white arrows point to unenveloped capsids]; Table 4). A similar phenotype (2- to 3-fold reduced envelopment) was

TABLE 2 Cytoplasmic and cell surface distribution of capsids produced by the gE− US9− double mutant F-gE/US9-GFP in SK-N-SH neurons[a]

Virus	No. of capsids (% of all capsids)			
	Unenveloped cytoplasmic	Partially enveloped cytoplasmic	Enveloped cytoplasmic	Cell surface virion
F-gE/US9-GFP-R	16 (3.2)	20 (3.9)	41 (8.0)	435 (85)
F-gE/US9-GFP	277 (51)	156 (29)	53 (10)	55 (10)

[a]EM images of 7 or 8 HSV-infected cells (that possessed large numbers of capsids) were analyzed by counting and characterizing the capsids.

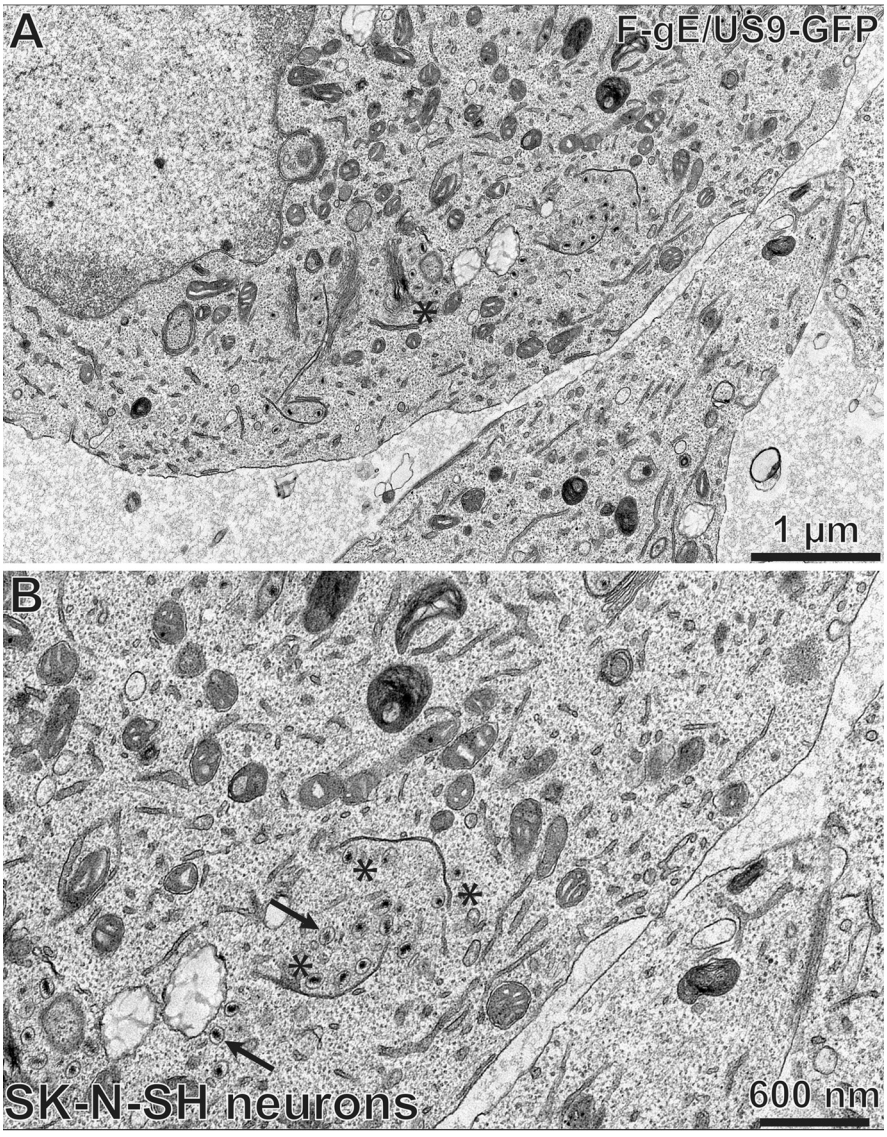

FIG 11 Electron micrographs of SK-N-SH neurons infected with the HSV F-gE/US9-GFP double mutant. SK-N-SH neurons growing on collagen-coated 60-mm dishes were differentiated for 10 days and then infected with the gE/US9 double mutant virus F-gE/US9-GFP at 5 PFU/cell for 18 h. The cells were fixed and processed for electron microscopy. These cells contained few enveloped virions on cell surfaces (A) and numerous unenveloped or only partially enveloped capsids in the cytoplasm (B). The black arrows indicate unenveloped capsids, and asterisks indicate capsids abutting tubular membranes. In panel A, there are capsids adjacent to a stack of membranes which is likely the Golgi apparatus.

seen with the gE-null mutant F-gEβ (Fig. 13E and F [white arrows show enveloped capsids]; Table 4), as observed previously for nonneuronal cell types (27). These modest differences between repaired viruses and the gE$^-$ or gE$^-$ US9$^-$ virus in nonneuronal cells were very different from the marked differences in mutant and repaired viruses in CAD neurons, where the majority of the capsids were not enveloped (gE$^-$ US9$^-$ mutant) or did not reach cell surfaces (gE$^-$ mutant). No substantial alterations in assembly were observed in HaCaT cells infected with the US9-null mutant, F-US9-GFP (Fig. 13D; Table 4). Some unenveloped virions were observed in these cells (Fig. 13D, white arrow), but not substantially more than in cells infected with the repaired virus, F-gE/US9-GFP-R (Table 4). We concluded that gE-null and gE$^-$ US9$^-$ mutants exhibit small defects in assembly (2- to 3-fold) in HaCaT cells. The US9-null mutant was not significantly different from repaired viruses in HaCaT cells. Therefore, both gE/gI and

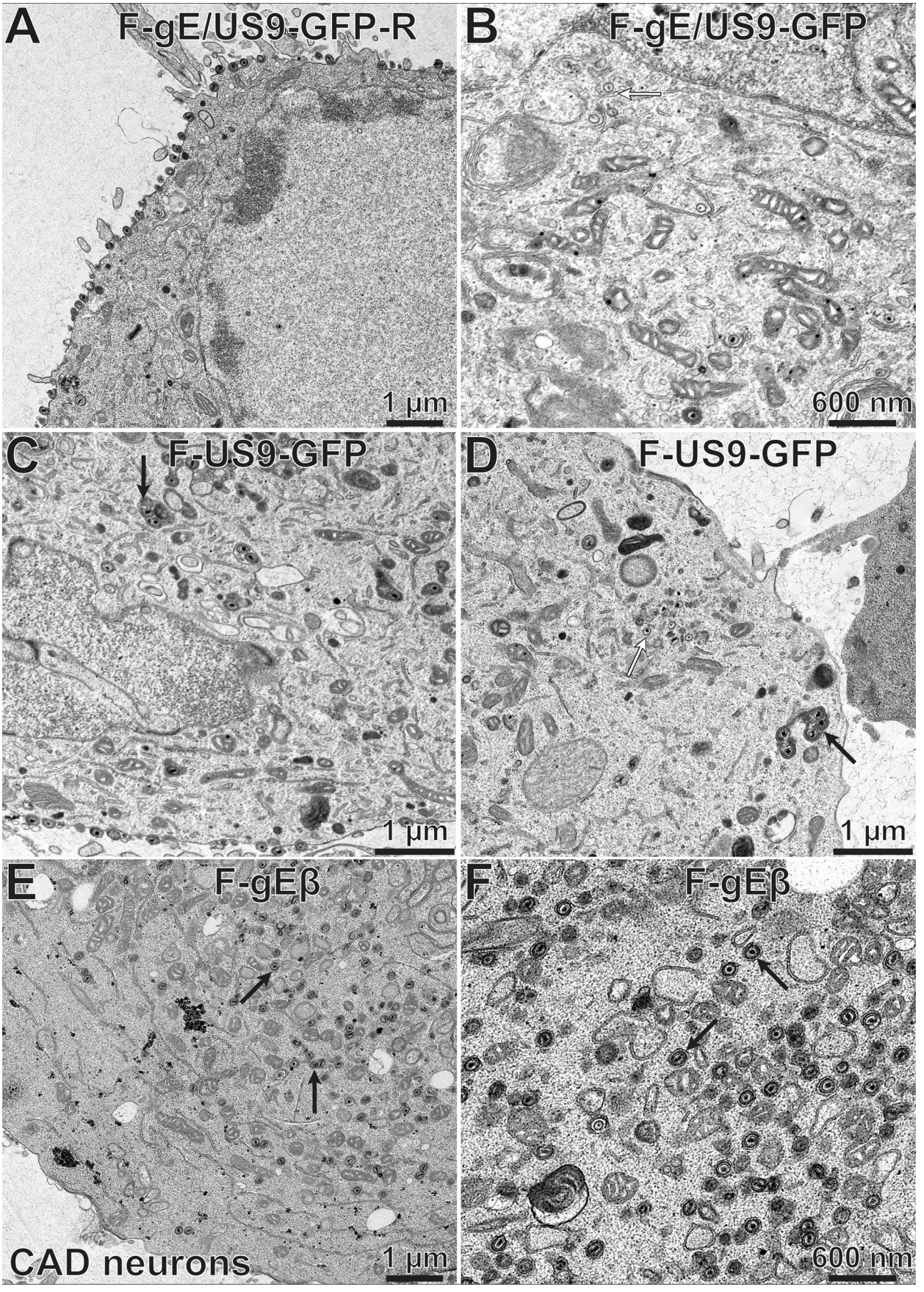
A
F-gE/US9-GFP-R
1 μm
B
F-gE/US9-GFP
600 nm
C
F-US9-GFP
1 μm
D
F-US9-GFP
1 μm
E
F-gEβ
CAD neurons
1 μm
F
F-gEβ
600 nm

TABLE 3 Cytoplasmic and cell surface distribution of capsids produced by the gE- and US9-null mutants, F-gEβ and F-US9-GFP[a]

Virus	No. of capsids (% of all capsids)			
	Unenveloped cytoplasmic	Partially enveloped cytoplasmic	Enveloped cytoplasmic	Cell surface virion
F-gE/US9-GFP-R	25 (4.3)	11 (1.9)	29 (5.1)	504 (88)
F-gE/US9-GFP	643 (63)	229 (22)	88 (8.6)	59 (5.8)
F-US9-GFP	422 (29)	202 (14)	82 (5.6)	733 (51)
F-gEβ	95 (7.8)	140 (12)	814 (67)	157 (13)

[a]EM images of sections of 9 to 13 HSV-infected cells were analyzed by counting and characterizing the capsids.

US9 are much more important for envelopment and sorting of virus particles in neurons than for those in nonneuronal cells.

DISCUSSION

Many previous studies on how HSV and PRV gE/gI and US9 promote axonal transport in neurons have focused on interactions between these viral proteins and kinesin motors that transport virus particles in axons and might promote movement of particles into axons to begin the process. PRV US9 binds to a kinesin-3 protein, KIF1A (15), and the HSV US9 and US11 proteins bind kinesin-1 proteins in pulldown experiments (22, 26). It was also suggested that HSV US9-null mutants have defects during anterograde transport, i.e., after virus entry into axons (39). However, our studies of both gE$^-$ and US9$^-$ single mutants and gE$^-$ US9$^-$ double mutants produced different conclusions: once HSV capsids or virions enter axons, their transport is normal, the kinetics of transport are not different from those for wild-type HSV, and there is no increased stalling (17). Similar observations were made with a PRV US9-null mutant (16). Those results, coupled with our observation that virus particles formed by gE$^-$ US9$^-$ double mutants do not enter proximal axons (17), suggest that gE/gI and gI act primarily in neuronal cell bodies to initiate anterograde transport before they reach axons. Kinesins might promote entry of virus particles into axons, but the studies here suggest a completely different model for how HSV gE/gI and US9 function to promote anterograde transport.

The results we report here suggest two mechanisms for how gE/gI and US9 might function. The first model, which we denote the assembly model, suggests that gE/gI and US9 promote assembly of enveloped particles in the cytoplasm and that this is a necessary first step for anterograde transport. The second mechanism, denoted the missorting model, is described below and suggests that both unenveloped and enveloped capsids are missorted such that these virus particles do not enter axons. Missorting was suggested by observations that the gE-null mutant produced enveloped particles but that these did not reach cell surfaces. The assembly model derives from observations that HSV gE$^-$ US9$^-$ double mutants showed an accumulation of unenveloped and partially enveloped capsids distributed in the cytoplasm. Given that the primary form of anterograde transport in CAD neurons involves enveloped virions (inside membrane vesicles), the absence of these enveloped virions in neurons infected with gE$^-$ US9$^-$ mutants can explain the reduced transport into axons that we observed.

One major problem with the assembly model relates to the many reports that HSV unenveloped capsids are a major form of virus particles that are transported in axons,

FIG 12 Electron micrographs of CAD neurons infected with F-gE/US9-GFP-R, F-gE/US9-GFP, F-US9-GFP, and F-gEβ. CAD neurons growing on collagen-coated 60-mm dishes were differentiated for 7 days and then infected with the repaired virus F-gE/US9-GFP-R (A), the double mutant F-gE/US9-GFP (B), a mutant lacking just US9 (F-US9-GFP) (C and D), or a mutant lacking just gE (F-gEβ) (E and F) at 20 PFU/cell. After 18 h, the cells were fixed and processed for electron microscopy. CAD neurons infected with F-gE/US9-GFP-R exhibited largely enveloped virions at the cell surface, while cells infected with F-gE/US9-GFP showed numerous unenveloped (white arrow in panel B) or partially enveloped capsids in the cytoplasm. CAD neurons infected with the US9 mutant F-US9-GFP exhibited numerous dense vesicles, frequently containing several capsids (black arrows in panels C and D), as well as unenveloped capsids (white arrow in panel D). CAD cells infected with the gE mutant F-gEβ exhibited primarily fully enveloped capsids in the cytoplasm (black arrows in panels E and F), with few virions on the cell surface.

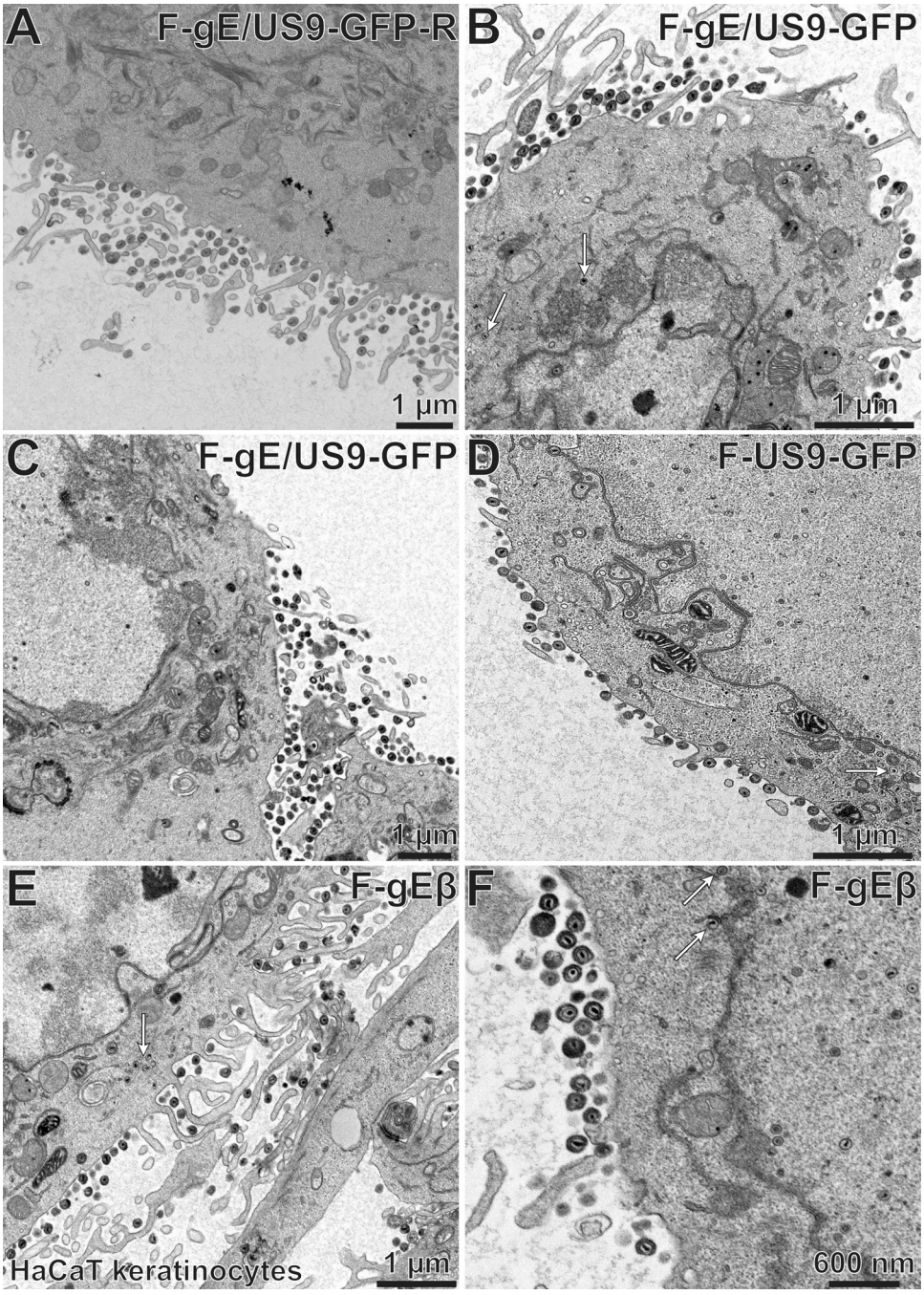

FIG 13 Electron micrographs of HaCaT cells infected with F-gE/US9-GFP-R, F-gE/US9-GFP, F-US9-GFP, or F-gEβ. HaCaT keratinocytes were grown on plastic 60-mm dishes and then infected with the repaired virus F-gE/US9-GFP-R (A), the double mutant F-gE/US9-GFP (B and C), the US9 mutant US9-GFP (D), or the gE mutant F-gEβ (E and F) at 15 PFU/cell. After 18 h, the cells were fixed and processed for electron microscopy. All four of these viruses produced largely cell surface virions, though there was some accumulation of unenveloped capsids (white arrows) with the F-gE/US9-GFP double mutant and the gE-null mutant (F-gEβ). No significant defects in assembly were observed with the US9 mutant (F-US9-GFP).

i.e., the so-called separate model of axonal transport (17, 35, 37, 38, 40–42). Others have argued that there is primarily anterograde transport of HSV enveloped particles (virions within membrane vesicles), i.e., so-called married transport (43, 44). If the separate mechanism is a major form of HSV anterograde transport and gE⁻ US9⁻ mutants accumulate unenveloped (separate) capsids, then one would assume that there should still be transport of these capsids, yet this is clearly not the case. We believe that both

TABLE 4 Cytoplasmic and cell surface distribution of capsids produced by gE$^-$ US9$^-$, gE-null, and US9-null mutants in HaCaT human keratinocytes[a]

Virus	No. of capsids (% of all capsids)			
	Unenveloped cytoplasmic	Partially enveloped cytoplasmic	Enveloped cytoplasmic	Cell surface virion
F-gE/US9-GFP-R	41 (5.9)	15 (2.1)	40 (5.7)	593 (85)
F-gE/US9-GFP	74 (15)	39 (7.7)	78 (15)	314 (62)
F-US9-GFP	63 (8.9)	7 (1.0)	43 (6.1)	591 (84)
F-gEβ	89 (16)	23 (4.1)	51 (9.2)	392 (71)

[a]EM images of sections of 8 to 11 HSV-infected cells were analyzed by counting and characterizing the capsids.

the separate and married HSV axonal transport mechanisms occur. The ratio of separate to married particles apparently depends upon the origin of the neurons being studied (primary neurons versus neuroblastomas, rat versus human, etc.) and how the transport is characterized, i.e., by using recombinant viruses expressing fluorescent proteins, staining with antibodies, or EM. In all of our recent and previous studies of SCG neurons infected with "two-color" recombinants expressing fluorescent viral proteins, there were mixtures of married and separate particles, with roughly equal numbers of each (17, 35). But here we found ~90% married particles in axons of differentiated CAD cells. Therefore, the neurons used to study this phenomenon can make a difference. If both the married and separate transport mechanisms occur, then we must explain the effects of gE/gI and US9 on both pathways. One potential explanation is that unenveloped capsids produced by gE$^-$ US9$^-$ mutants are missing other viral proteins which interact with kinesins or other sorting proteins necessary to access axons.

However, a better explanation for why unenveloped capsids are not transported into axons in gE$^-$ US9$^-$ mutant-infected SCG neurons might be described by the missorting model. We observed that most gE$^-$ US9$^-$ mutant capsids that accumulate are adhered to or nestled up against membranes in the cytoplasm (Fig. 7B and C and 11B). We know that gE/gI and likely US9 accumulate in the TGN, a site of virus assembly (29). gE/gI and US9 share TGN sorting motifs (Fig. 1). We also know that gE/gI sorts virus particles to epithelial cell-cell junctions (6, 30). Therefore, the loss of gE/gI and US9 in neurons might lead to misrouting of both HSV capsids and enveloped virions such that virus particles do not enter axons. Since gE/gI and US9 are likely to be present in the membranes to which enveloped capsids are bound, gE/gI and US9 might influence the sorting of unenveloped capsids into axons by some unknown mechanism. However, the sorting of enveloped virions might also be affected, as gE/gI and US9 would be present in the vesicles that enclose these virions. Support for the missorting model came from studies of the gE-null mutant in CAD neurons, in which enveloped virions accumulated in the cytoplasm but did not reach cell surfaces. We concluded that these enveloped particles must be missorted, confined to the cytoplasm, and not able to reach cell surfaces.

We have demonstrated that the loss of both HSV gE and US9 produces two effects in the cytoplasm of neurons, namely, (i) inhibiting envelopment so that married particles are not produced and (ii) affecting sorting of both married and separate particles into axons. It is very interesting that the loss of gE/gI and US9 has such profound effects on assembly and sorting in neurons but not in nonneuronal cells.

MATERIALS AND METHODS

Cells. Vero cells were propagated in Dulbecco's modified Eagle's medium (DMEM; Invitrogen) with 8% fetal bovine serum (FBS) (ISC BioExpress, Kaysville, UT). HaCaT cells, a spontaneously transformed keratinocyte line, were grown in DMEM containing 10% fetal bovine serum.

Viruses. An HSV-1 strain in which β-galactosidase sequences were used to replace the US8 (gE) and US8A genes and a repaired version of the F-gEβ virus in which gE was repaired (F-gEβ-R) were described previously (4). HSV-1 F-US9-GFP, in which green fluorescent protein (GFP) sequences replace the US9 gene, and a repaired virus, FUS9-GFP-R, were described previously (9). An HSV-1 double mutant (F-gE/US9-GFP) in which both the gE (US8) and US9 genes were replaced with enhanced green fluorescent protein (EGFP) sequences and a repaired version of this virus were described previously (17). This mutant also lacked

US8A. Wild-type (WT) HSV-1 GS2843, which expresses VP26-mRFP and gB-GFP (34), and a virus derived from this strain that has a deletion in the gE (US8) and US9 genes (17) were described previously. All HSV recombinants were derived from HSV-1 strain F, and all were constructed using bacterial artificial chromosomes, except for F-gEβ, which was constructed by homologous recombination.

Neuronal cell cultures. SK-N-SH neuroblastoma cells (American Type Culture Collection) were propagated and differentiated as described previously (37). Note that the SK-N-SH cell line was derived by passaging the cells as follows. Cells were dislodged from plastic dishes by shaking or hitting the plates so as to obtain largely neuronal cells and leave behind epithelioid cells in the cultures that remained attached to plastic. This was done 5 times, producing cells with fewer epithelioid cells. CAD cells, a derivative of a mouse catecholaminergic central nervous system cell line, were a kind gift from Greg Smith, Northwestern University Medical School, Chicago, IL (34), and were maintained in DMEM/F12 containing 10% FBS and passaged by gentle dissociation with sodium citrate buffer (134 mm KCl, 15 mM sodium citrate, pH 7.3 to 7.4). Differentiation of CAD cells was achieved by plating cells on poly-D-lysine (30 μg/ml)- and laminin (2 μg/ml)-coated glass coverslips in differentiation medium (DMEM/F12 containing 0.5% fetal bovine serum, 10 μM 3-isobutyl-1-methylxanthine [IBMX], 150 μM dibutyryl-cyclic AMP [dbcAMP], and 1 ng/ml nerve growth factor [NGF] [2.5S; Invitrogen]). After 2 days, the IBMX and dbcAMP were removed. The cells were differentiated for 7 to 10 days before being infected with HSV. Rat embryonic superior cervical ganglion (SCG) neurons were produced as described previously (17).

Growth of HSV in CAD cells. CAD cells were plated in triplicate (for each virus being tested) in 6-well (10 cm^2) dishes coated with poly-D-lysine/laminin and then differentiated as described above. On day 8 postdifferentiation, the cells were infected with virus at 20 PFU/cell for 2 h, and then the cells were washed twice with differentiation medium and overlaid with differentiation medium. After various times, the cells were harvested in medium by scraping the cells from dishes, sonicated briefly before virus titration using Vero cell monolayers infected with virus, and then overlaid with 0.2% human gamma globulin.

Immunofluorescence imaging of HSV-infected neurons. CAD cells were plated on poly-D-lysine (30 μg/ml)- and laminin (2 μg/ml)-coated glass coverslips, infected with HSV for 12 to 18 h, and then washed and fixed by addition of phosphate-buffered saline (PBS), pH 7.4, containing 4% paraformaldehyde for 20 min at 20°C. The cells were then permeabilized using 0.5% sodium deoxycholate for 10 min and were sequentially blocked for 20 min in 5% normal goat serum and for 1 h in 0.3 mg/ml sheep anti-mouse IgG to reduce mouse-on-mouse nonspecific IgG binding to background levels. CAD cells were incubated with primary antibodies in PBS containing 0.1% Tween 20 and 5% normal goat serum for 1 h, washed in PBS containing 0.1% Tween 20 five times, and incubated with secondary fluorescent antibodies in PBS containing 0.1% Tween 20 for 1 h. For some samples, 300 nM 4′,6-diamidino-2-phenylindole (DAPI) was added for 5 min to stain nuclei. Microscopy was performed at the Oregon Health and Sciences University's Advanced Light Microscopy Core, using a high-resolution wide-field Core DV system (Applied Precision). This system is an Olympus IX71 inverted microscope with a proprietary *xyz* stage, a solid-state module for fluorescence, and a Nikon Coolsnap ES2 HQ camera. Images were acquired as z-stacks in a 1,024- by 1,024-pixel format with a 60× (numerical aperture, 1.42) Plan Apo N objective in three channels: 435, 549, and 649 nm. The images were deconvolved with the appropriate optical transfer function (OTF) by using an iterative algorithm of 10 iterations. After deconvolution, images were processed with FIJI (ImageJ). For visualization of VP26 and gB puncta, at least 5 images (10,560 μm^2) per slide were captured with a minimum of 9 0.2-μm z-sections. These images were analyzed using a minimum intensity threshold chosen based on matched uninfected control cells that yielded no VP26 and gB fluorescence.

Capsid quantification. To quantify capsids in immunofluorescence imaging experiments, deconvolved image data were analyzed in Bitplane's Imaris software v8.3.1. Briefly, z-stacks were used to generate volumes and surfaces, and capsids (VP26-mRFP) were counted by use of the Spots function. Spot size was determined by averaging individual capsid signals from the residual input stuck to the glass coverslip. Nuclear capsids were excluded from the count by using the glycoprotein signal to define the cytoplasm.

Antibodies. Rabbit polyclonal anti-VP26 antibody (45) was kindly provided by Prashant Desai (Johns Hopkins University, Baltimore, MD). A mouse anti-gB monoclonal antibody (MAb) (SS10) (46) was kindly provided by Gary Cohen (University of Pennsylvania, Philadelphia, PA). DyLight fluorescent secondary antibodies were purchased from Jackson ImmunoResearch.

Electron microscopy. CAD cells were plated in collagen-coated 60-mm plastic dishes (Celltreat; Greiner Bio-One) at 1.3 × 10^6/dish and then allowed to grow to ~80% confluence before being differentiated as described above for 7 to 10 days. In some experiments, CAD cells were plated in 12-well dishes with 22-mm glass coverslips coated with lysine/laminin at 170,000 cells per well and then differentiated. CAD cells were infected with virus at 20 PFU/cell by incubating cells and virus for 2 h and then removing the inoculum, washing the cells, and incubating the cells in differentiation medium for 15 to 18 h. Cells were washed once in 100 mM sodium cacodylate buffer, pH 7.2, and then fixed in Karnofsky's solution (cacodylate buffer containing 2% [wt/vol] paraformaldehyde and 2.5% [wt/vol] glutaraldehyde) for 30 min at room temperature, scraped into this solution, centrifuged into Eppendorf tubes, and stored at 4°C before processing for EM. Rat embryonic SCG neurons were spotted in 100 μl of growth medium onto lysine/laminin-coated 13-mm Thermanox coverslips at 80,000 SCG neurons/coverslip and grown as previously described. After 10 days, the neurons were infected with HSV at 2 PFU/cell for 2 h, and then the inoculum was removed and the cells washed once. After 18 h, the neurons were washed and fixed as described above. SK-N-SH cells were plated onto collagen-coated 60-mm dishes (as for CAD cells) and allowed to grow to 60% confluence before the cells were differentiated as

described previously (37). Differentiated SK-N-SH cells were infected with HSV at 2 PFU/cell and fixed at 18 h postinfection as described above. HaCaT cells were grown in 60-mm plastic dishes until 70 to 80% confluence and then infected with HSV at 15 PFU/cell by allowing virus adsorption for 2 h and then removing the inoculum and washing the cells. At 18 h postinfection, the cells were washed, fixed, and scraped from the plastic into Karnofsky's solution as described above. Following fixation, samples were rinsed in 0.1 M sodium cacodylate buffer, incubated in reduced osmium tetroxide (1.5% potassium ferrocyanide in 2% OsO_4), rinsed in water, and stained *en bloc* with aqueous 0.5% uranyl acetate. Following the uranyl acetate incubation, samples were dehydrated in an aqueous series of 50%, 75%, and 95% acetone, followed by two exchanges in 100% acetone. Epon resin infiltration was facilitated by incubation in a 1:1 solution of 100% acetone and freshly made Epon resin, followed by 4 exchanges in 100% freshly made Epon resin. Samples were transferred into embedding capsules (Beem) filled with freshly made Epon resin and cured at 60°C for 36 h. Thin sections (70 nm) obtained from the block face were imaged at 80 kV on an FEI-Tecnai 12 system interfaced to a digital camera and associated software (Advanced Microscopy Techniques, Danvers, MA).

ACKNOWLEDGMENTS

We thank Tiffani Howard for her skilled surgery to remove rat embryos from pregnant rats and for teaching others how to carry this out. We are grateful to Aurelie Snyder for excellent support for deconvolution experiments in the OHSU Advance Light Microscopy Core at the Jungers Center, OHSU. This work could not have been completed without mentoring from Frank Graham, who remains a pioneer in virology.

These studies were supported by a grant from the National Institutes of Health (grant R01 EY018755 to D.C.J.).

REFERENCES

1. Smith G. 2012. Herpesvirus transport to the nervous system and back again. Annu Rev Microbiol 66:153–176. https://doi.org/10.1146/annurev-micro-092611-150051.
2. Johnson DC, Baines JD. 2011. Herpesviruses remodel host membranes for virus egress. Nat Rev Microbiol 9:382–394. https://doi.org/10.1038/nrmicro2559.
3. Howard PW, Wright CC, Howard T, Johnson DC. 2014. Herpes simplex virus gE/gI extracellular domains promote axonal transport and spread from neurons to epithelial cells. J Virol 88:11178–11186. https://doi.org/10.1128/JVI.01627-14.
4. Dingwell KS, Brunetti CR, Hendricks RL, Tang Q, Tang M, Rainbow AJ, Johnson DC. 1994. Herpes simplex virus glycoproteins E and I facilitate cell-to-cell spread in vivo and across junctions of cultured cells. J Virol 68:834–845.
5. Wisner T, Brunetti C, Dingwell K, Johnson DC. 2000. The extracellular domain of herpes simplex virus gE is sufficient for accumulation at cell junctions but not for cell-to-cell spread. J Virol 74:2278–2287. https://doi.org/10.1128/JVI.74.5.2278-2287.2000.
6. Johnson DC, Webb M, Wisner TW, Brunetti C. 2001. Herpes simplex virus gE/gI sorts nascent virions to epithelial cell junctions, promoting virus spread. J Virol 75:821–833. https://doi.org/10.1128/JVI.75.2.821-833.2001.
7. Dingwell KS, Doering LC, Johnson DC. 1995. Glycoproteins E and I facilitate neuron-to-neuron spread of herpes simplex virus. J Virol 69:7087–7098.
8. Wang F, Zumbrun EE, Huang J, Si H, Makaroun L, Friedman HM. 2010. Herpes simplex virus type 2 glycoprotein E is required for efficient virus spread from epithelial cells to neurons and for targeting viral proteins from the neuron cell body into axons. Virology 405:269–279. https://doi.org/10.1016/j.virol.2010.06.006.
9. Polcicova K, Biswas PS, Banerjee K, Wisner TW, Rouse BT, Johnson DC. 2005. Herpes keratitis in the absence of anterograde transport of virus from sensory ganglia to the cornea. Proc Natl Acad Sci U S A 102:11462–11467. https://doi.org/10.1073/pnas.0503230102.
10. McGraw HM, Awasthi S, Wojcechowskyj JA, Friedman HM. 2009. Anterograde spread of herpes simplex virus type 1 requires glycoprotein E and glycoprotein I but not Us9. J Virol 83:8315–8326. https://doi.org/10.1128/JVI.00633-09.
11. Enquist LW, Husak PJ, Banfield BW, Smith GA. 1998. Infection and spread of alphaherpesviruses in the nervous system. Adv Virus Res 51:237–347. https://doi.org/10.1016/S0065-3527(08)60787-3.
12. Enquist LW, Tomishima MJ, Gross S, Smith GA. 2002. Directional spread of an alpha-herpesvirus in the nervous system. Vet Microbiol 86:5–16. https://doi.org/10.1016/S0378-1135(01)00486-2.
13. Snyder A, Polcicova K, Johnson DC. 2008. Herpes simplex virus gE/gI and US9 proteins promote transport of both capsids and virion glycoproteins in neuronal axons. J Virol 82:10613–10624. https://doi.org/10.1128/JVI.01241-08.
14. Lyman MG, Feierbach B, Curanovic D, Bisher M, Enquist LW. 2007. PRV Us9 directs axonal sorting of viral capsids. J Virol 81:11363–11371. https://doi.org/10.1128/JVI.01281-07.
15. Kramer T, Greco TM, Taylor MP, Ambrosini AE, Cristea IM, Enquist LW. 2012. Kinesin-3 mediates axonal sorting and directional transport of alphaherpesvirus particles in neurons. Cell Host Microbe 12:806–814. https://doi.org/10.1016/j.chom.2012.10.013.
16. Daniel GR, Sollars PJ, Pickard GE, Smith GA. 2015. Pseudorabies virus fast axonal transport occurs by a pUS9-independent mechanism. J Virol 89:8088–8091. https://doi.org/10.1128/JVI.00771-15.
17. Howard PW, Howard TL, Johnson DC. 2013. Herpes simplex virus membrane proteins gE/gI and US9 act cooperatively to promote transport of capsids and glycoproteins from neuron cell bodies into initial axon segments. J Virol 87:403–414. https://doi.org/10.1128/JVI.02465-12.
18. Kratchmarov R, Kramer T, Greco TM, Taylor MP, Ch'ng TH, Cristea IM, Enquist LW. 2013. Glycoproteins gE and gI are required for efficient KIF1A-dependent anterograde axonal transport of alphaherpesvirus particles in neurons. J Virol 87:9431–9440. https://doi.org/10.1128/JVI.01317-13.
19. Taylor MP, Kramer T, Lyman MG, Kratchmarov R, Enquist LW. 2012. Visualization of an alphaherpesvirus membrane protein that is essential for anterograde axonal spread of infection in neurons. mBio 3:e00063-12. https://doi.org/10.1128/mBio.00063-12.
20. Bacchetti S, Graham FL. 1977. Transfer of the gene for thymidine kinase to thymidine kinase-deficient human cells by purified herpes simplex viral DNA. Proc Natl Acad Sci U S A 74:1590–1594. https://doi.org/10.1073/pnas.74.4.1590.
21. Wolfstein A, Nagel CH, Radtke K, Dohner K, Allan VJ, Sodeik B. 2006. The inner tegument promotes herpes simplex virus capsid motility along microtubules in vitro. Traffic 7:227–237. https://doi.org/10.1111/j.1600-0854.2005.00379.x.
22. Diefenbach RJ, Davis A, Miranda-Saksena M, Fernandez MA, Kelly BJ, Jones CA, LaVail JH, Xue J, Lai J, Cunningham AL. 2015. The basic domain of herpes simplex virus 1 pUS9 recruits kinesin-1 to facilitate egress from neurons. J Virol 90:2102–2111. https://doi.org/10.1128/JVI.03041-15.
23. Hirokawa N, Niwa S, Tanaka Y. 2010. Molecular motors in neurons: transport mechanisms and roles in brain function, development, and disease. Neuron 68:610–638. https://doi.org/10.1016/j.neuron.2010.09.039.
24. Hirokawa N, Tanaka Y. 2015. Kinesin superfamily proteins (KIFs): various

functions and their relevance for important phenomena in life and diseases. Exp Cell Res 334:16–25. https://doi.org/10.1016/j.yexcr.2015.02.016.
25. Salogiannis J, Reck-Peterson SL. 2017. Hitchhiking: a non-canonical mode of microtubule-based transport. Trends Cell Biol 27:141–150. https://doi.org/10.1016/j.tcb.2016.09.005.
26. Diefenbach RJ, Miranda-Saksena M, Diefenbach E, Holland DJ, Boadle RA, Armati PJ, Cunningham AL. 2002. Herpes simplex virus tegument protein US11 interacts with conventional kinesin heavy chain. J Virol 76:3282–3291. https://doi.org/10.1128/JVI.76.7.3282-3291.2002.
27. Farnsworth A, Goldsmith K, Johnson DC. 2003. Herpes simplex virus glycoproteins gD and gE/gI serve essential but redundant functions during acquisition of the virion envelope in the cytoplasm. J Virol 77:8481–8494. https://doi.org/10.1128/JVI.77.15.8481-8494.2003.
28. Farnsworth A, Wisner TW, Johnson DC. 2007. Cytoplasmic residues of herpes simplex virus glycoprotein gE required for secondary envelopment and binding of tegument proteins VP22 and UL11 to gE and gD. J Virol 81:319–331. https://doi.org/10.1128/JVI.01842-06.
29. McMillan TN, Johnson DC. 2001. Cytoplasmic domain of herpes simplex virus gE causes accumulation in the *trans*-Golgi network, a site of virus envelopment and sorting of virions to cell junctions. J Virol 75:1928–1940. https://doi.org/10.1128/JVI.75.4.1928-1940.2001.
30. Wisner TW, Johnson DC. 2004. Redistribution of cellular and herpes simplex virus proteins from the *trans*-Golgi network to cell junctions without enveloped capsids. J Virol 78:11519–11535. https://doi.org/10.1128/JVI.78.21.11519-11535.2004.
31. Farnsworth A, Johnson DC. 2006. Herpes simplex virus gE/gI must accumulate in the *trans*-Golgi network at early times and then redistribute to cell junctions to promote cell-cell spread. J Virol 80:3167–3179. https://doi.org/10.1128/JVI.80.7.3167-3179.2006.
32. Stylianou J, Maringer K, Cook R, Bernard E, Elliott G. 2009. Virion incorporation of the herpes simplex virus type 1 tegument protein VP22 occurs via glycoprotein E-specific recruitment to the late secretory pathway. J Virol 83:5204–5218. https://doi.org/10.1128/JVI.00069-09.
33. McGeoch DJ, Dolan A, Donald S, Rixon FJ. 1985. Sequence determination and genetic content of the short unique region in the genome of herpes simplex virus type 1. J Mol Biol 181:1–13. https://doi.org/10.1016/0022-2836(85)90320-1.
34. Antinone SE, Zaichick SV, Smith GA. 2010. Resolving the assembly state of herpes simplex virus during axon transport by live-cell imaging. J Virol 84:13019–13030. https://doi.org/10.1128/JVI.01296-10.
35. Wisner TW, Sugimoto K, Howard PW, Kawaguchi Y, Johnson DC. 2011. Anterograde transport of herpes simplex virus capsids in neurons by both separate and married mechanisms. J Virol 85:5919–5928. https://doi.org/10.1128/JVI.00116-11.
36. Farnsworth A, Wisner TW, Webb M, Roller R, Cohen G, Eisenberg R, Johnson DC. 2007. Herpes simplex virus glycoproteins gB and gH function in fusion between the virion envelope and the outer nuclear membrane. Proc Natl Acad Sci U S A 104:10187–10192. https://doi.org/10.1073/pnas.0703790104.
37. Snyder A, Wisner TW, Johnson DC. 2006. Herpes simplex virus capsids are transported in neuronal axons without an envelope containing the viral glycoproteins. J Virol 80:11165–11177. https://doi.org/10.1128/JVI.01107-06.
38. Snyder A, Bruun B, Browne HM, Johnson DC. 2007. A herpes simplex virus gD-YFP fusion glycoprotein is transported separately from viral capsids in neuronal axons. J Virol 81:8337–8340. https://doi.org/10.1128/JVI.00520-07.
39. Miranda-Saksena M, Boadle RA, Diefenbach RJ, Cunningham AL. 2015. Dual role of herpes simplex virus 1 pUS9 in virus anterograde axonal transport and final assembly in growth cones in distal axons. J Virol 90:2653–2663. https://doi.org/10.1128/JVI.03023-15.
40. Penfold ME, Armati P, Cunningham AL. 1994. Axonal transport of herpes simplex virions to epidermal cells: evidence for a specialized mode of virus transport and assembly. Proc Natl Acad Sci U S A 91:6529–6533. https://doi.org/10.1073/pnas.91.14.6529.
41. Miranda-Saksena M, Armati P, Boadle RA, Holland DJ, Cunningham AL. 2000. Anterograde transport of herpes simplex virus type 1 in cultured, dissociated human and rat dorsal root ganglion neurons. J Virol 74:1827–1839. https://doi.org/10.1128/JVI.74.4.1827-1839.2000.
42. Cunningham A, Miranda-Saksena M, Diefenbach R, Johnson D. 2013. Letter in response to: making the case: married versus separate models of alphaherpes virus anterograde transport in axons. Rev Med Virol 23:414–418. https://doi.org/10.1002/rmv.1760.
43. Antinone SE, Smith GA. 2010. Retrograde axon transport of herpes simplex virus and pseudorabies virus: a live-cell comparative analysis. J Virol 84:1504–1512. https://doi.org/10.1128/JVI.02029-09.
44. Negatsch A, Granzow H, Maresch C, Klupp BG, Fuchs W, Teifke JP, Mettenleiter TC. 2010. Ultrastructural analysis of virion formation and intraaxonal transport of herpes simplex virus type 1 in primary rat neurons. J Virol 84:13031–13035. https://doi.org/10.1128/JVI.01784-10.
45. Desai P, DeLuca NA, Glorioso JC, Person S. 1993. Mutations in herpes simplex virus type 1 genes encoding VP5 and VP23 abrogate capsid formation and cleavage of replicated DNA. J Virol 67:1357–1364.
46. Bender FC, Samanta M, Heldwein EE, de Leon MP, Bilman E, Lou H, Whitbeck JC, Eisenberg RJ, Cohen GH. 2007. Antigenic and mutational analyses of herpes simplex virus glycoprotein B reveal four functional regions. J Virol 81:3827–3841. https://doi.org/10.1128/JVI.02710-06.